Shear and moment transfer at column-slab connections

Scott D. B. Alexander

COWI North America, Canada

Abstract

The Strip Model describes a load path for the transfer of vertical shear between a slab and column. The model is easily adapted to design but its application to the analysis of specimens tested under combined shear and moment is less clear. This paper provides a brief description of the Strip Model, updates the model to include size effect, and shows how it can be applied to interior and edge column-slab connections transferring combinations of shear and moment.

Keywords

Columns, connections, punching shear, reinforced concrete, shear strength, slabs, structural design.

1 Introduction

The Strip Model for slab punching shear, originally called the Bond Model (Alexander and Simmonds, 1992), describes an internal distribution for the transfer of vertical load between a two-way slab and column. The model may be considered an extension of the Strip Method of Design (Hillerborg, 1975). The Strip Method allows a designer to define a load distribution that rigorously satisfies equilibrium at all points in a slab and to reinforce the slab for the bending moments that are the consequence of that load distribution. The Strip Method as developed by Hillerborg does not address shear strength.

The Strip Model for slab punching shear is consistent with the Strip Method for flexural design but is focused on a particular problem: the development of an internal load distribution for shear transfer at concentrated loads that does not violate either shear or flexural strength limits at any point. This internal load distribution is derived from subdividing the slab into regions dominated by slender flexural behavior (B-regions) and regions dominated by deep beam behavior (D-regions). The result is a model for shear transfer that can be verified by direct measurement (Alexander et al., 1995).

The distinguishing characteristic of a B- or D-region is the predominant mechanism of moment gradient (i.e. shear transfer). In a slender beam, moment gradient is mostly the result of a varying flexural tension force acting on a more or less constant moment arm. Such behavior is called **beam action**. In a deep beam, moment gradient results from a constant tensile force acting on a varying moment arm. This behavior is called **arching action**.

It is appropriate to describe shear transfer by beam action in terms of an average shear stress acting on the cross-section. A reasonable design strategy for slender members is to limit the average shear stress to some critical value; however, an average shear stress does not model the behavior in a D-region. D-regions are more correctly modeled using strut-and-tie.

Column-slab connections exhibit the characteristics of both B- and D-regions. Tests show that radial arching action is an important mechanism of shear transfer between a slab and a column, suggesting that column-slab connections should be considered D-regions. In the circumferential direction, however, column-slab connections behave more like B-regions.

This paper provides a brief summary of the mechanics of the strip model and extends the model to account for size effect. It then introduces the concepts of non-proportional loading and shows how these are used to describe the transfer of shear moment at a column-slab connection.

2 Strip model for concentric punching

2.1 Internal load distribution

The Strip Model divides the slab into radial strips and plate quadrants, as shown in Fig. 1. No load can reach the column without passing through one of the radial strips. Within each radial strip shear is carried to the column by arching action. This is visualized as a curved arch, with maximum slope at the face of the column as shown in Fig. 2. The quadrants of two-way slab are fundamentally slender flexural elements, which means shear transfer across the boundary between a strip and its adjacent quadrant of plate is through the two-way plate equivalent of beam action.

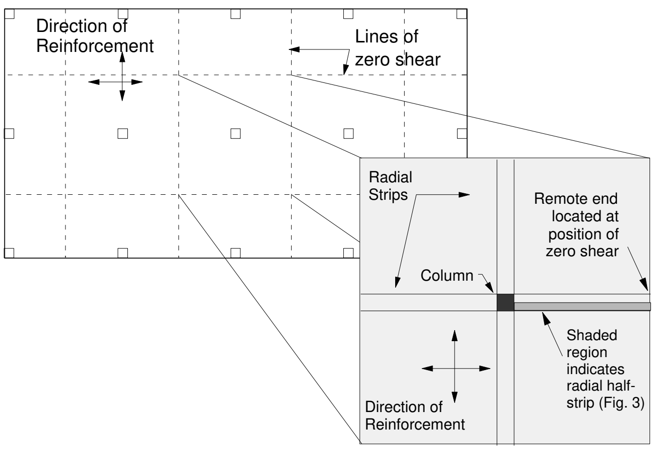

Figure 1: Geometry of Strip Model.

Consider the compression arch shown in Fig. 2. The compression force in the arch is approximately constant throughout. At the column face, the vertical component of the arch accounts for the shear transferred to the column; the horizontal component provides a flexural compression.

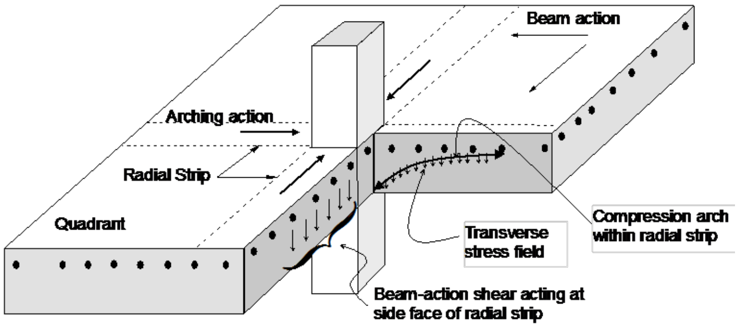

Figure 2: Beam and arching action at column-slab connection.

Moving away from the column, the slope of the arch decreases. Vertical equilibrium of the arch requires that there be a transverse stress field. The transverse stress field is internal and is generated by the two-way plate equivalent of beam action shear acting in a direction perpendicular to the arch. Thus, the model is of the interaction between the slender quadrants of plate and the radial strips acting as deep beams.

Figure 3 shows a free body diagram of half of a radial strip. The half-strip is loaded on its side face by a combination of plate bending moment, m_n, torsional moment, m_t, and shear, v. The strip is supported by a vertical reaction, P_s, at the column-supported end and bending moments, M_{neg} and M_{pos}, at the column and remote ends of the strip, respectively.

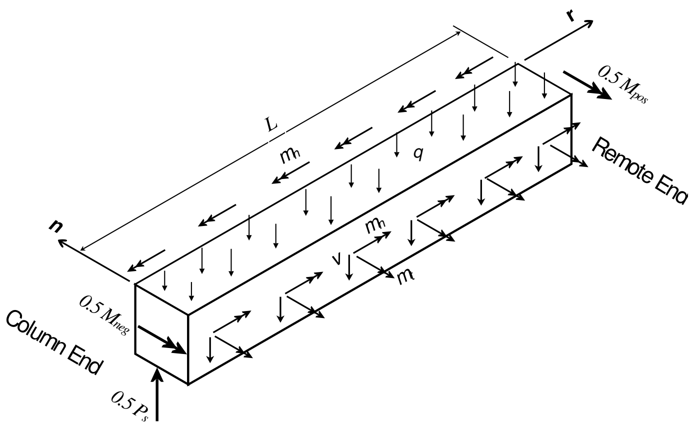

Figure 3: Forces on radial half-strip.

The internal vertical shear at any point along the side face of a radial strip is a function of the gradients of bending and torsional moments at that point. Alexander and Simmonds (1992) and Afhami et al. (1998) examine the various components of this internal shear in some detail to justify the simplified free body diagrams of radial strips at ultimate load, shown in Fig. 4. The loading term, w, is the limiting one-way shear that can be carried by the slab. An internal radial strip, such as those shown in Fig. 1, is loaded on two faces; hence the total distributed line load on the strip is $2w$. At an edge column, a spandrel strip running parallel to the free edge of the slab would be loaded on only one side and so would be subject to a line load of w.

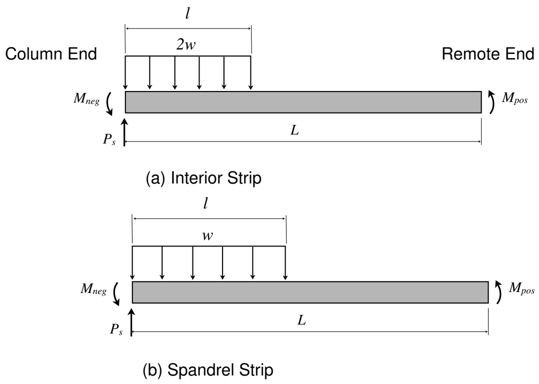

Figure 4: Simplified loading on radial strip.

The flexural strength of the radial strip, M_s, is the sum of the negative and positive flexural capacities, M_{neg} and M_{pos}, at the ends of the strip. The loaded length of the strip is l and the total load carried by one strip is P_s, termed the **nominal capacity** of a strip. Equilibrium for an internal radial strip requires that:

$$l = \sqrt{\frac{M_s}{w}} \tag{1}$$

$$P_s = 2\sqrt{M_s w} \tag{2}$$

The corresponding equations for a spandrel strip are:

$$l = \sqrt{\frac{2M_s}{w}} \tag{3}$$

$$P_s = \sqrt{2M_s w} \tag{4}$$

The total load that can be delivered to the column is simply the summation of the individual strip contributions.

$$P_{col} = \sum P_s \tag{5}$$

While the load distribution described above is certainly a simplification of reality, it is nevertheless realistic. The radial strips are parallel to the stiff directions of the reinforcing mat. Alexander et al. (1995) and Afhami et al. (1998) show that bending moment gradients perpendicular to the side faces of radial strips, estimated from strain gauge measurements, account for the measured column reaction over a considerable range of loading. Using non-linear finite elements, Afhami et al. (1998) show that yielding of flexural reinforcement through the column results in a stepped distribution of internal shear along the side face of a radial strip, consistent with what is shown in Fig. 4.

Earlier work (Alexander and Simmonds, 1992) examines a limited data set of 116 concentrically loaded interior column-slab connections from eight sources, six with simply supported edges and two with rotationally restrained edges. The flexural capacities are strictly limited to those of the strip of slab defined by the width of the column.

$$M_{neg} = \rho_{neg} \times f_y \times j \times c \times d^2 \tag{6a}$$

$$M_{pos} = \rho_{pos} \times f_y \times j \times c \times d^2 \tag{6b}$$

$$j = 1 - \frac{\rho f_y}{1.7 f_c'} \tag{6c}$$

$$M_s = M_{pos} + M_{neg} \tag{6d}$$

Consistent with the assumption of slender flexural behavior, the loading term w is taken as the unit one-way shear strength of the slab. Based on ACI 318-14 (ref), w is given by:

$$w = d \times 0.17\sqrt{f'_c\,(MPa)} = d \times 2\sqrt{f'_c\,(psi)} \tag{7}$$

where d is the flexural depth of the slab and f_c' is the specified concrete strength.

Alexander and Simmonds (1992) report an average ratio of test load to calculated load of 1.29 with a coefficient of variation of 12.3%. On the same body of test results, the ratio of test load to the load predicted by ACI code is 1.56 with a coefficient of variation of 26.5%.

To illustrate a typical set of calculations used to analyze these tests, consider a hypothetical interior column-slab punching test specimen. The slab measures 2.33 m (7 ft) square, centered on a 400 mm (15.75 in) square column. The slab has 1% top reinforcement each way based on an average flexural depth of 130 mm (5.12 in). The yield strength of the reinforcement is 400 MPa (58 ksi) and the concrete strength is 30 MPa (4350 psi). The slab is loaded on its perimeter. There is no rotational restraint at the boundary (i.e. $M_{pos} = 0$).

From Equations (6a) through (6d):

$$M_s = 1\% \times 400MPa \times \left(1 - \frac{1\% \times 400MPa}{1.7 \times 30MPa}\right) \times 400\text{ mm} \times (130\text{ mm})^2 = 24.9\text{ kN}\cdot\text{m};\ (18.4\text{ ft}\cdot\text{kips})$$

From Equation (7), $w = 130\text{ mm} \times 0.17 \times \sqrt{30\text{ MPa}} = 121\ N/\text{mm}$; (8.29 kips/ft).

From Equation (2), $P_s = 2\sqrt{24.9 \times 121} = 110$ kN (24.7 kips). Because there are four strips framing into the column, Equation (5) gives a total load of 440 kN (98.8 kips).

Note that even though the top reinforcing mat will have two values of d, one for each layer of reinforcement. The average value of d, measured to the middle of the mat, is used for all calculations. One could consider the different values of d but this is needlessly complicated. The larger value of d for flexure always pairs with the smaller value of d for the loading term, w, and vice versa.

2.2 Size effect

A shortcoming of the data set used by Alexander and Simmonds (1992) is the limited range of flexural depth. The deepest slab had a flexural depth of 200 mm (7.9 in). Forty-two of the tests were on small-scale specimens with flexural depths less than 55 mm (2.2 in).

To address this shortcoming, a subset of 257 specimens from the ACI 445 Punching Shear Databank (Ospina et al., 2011) is used. The subset has results from 38 separate sources. Specimens are simply supported (i.e. $M_{pos} = 0$), steel reinforced, with either square or circular columns. While the dataset still contains a large number of small-scale specimens (39 with flexural depth 65 mm [2.6 in] or less), it has better representation of deeper slabs (29 with flexural depths over 140 mm [5.5 in]).

Figure 5 shows distributions of the ratio of test load to calculated load with respect to flexural depth. In Fig. 5(a) the calculated loads are nominal capacities based on the ACI code. The average ratio of test load to calculated load is 1.45 and the coefficient of variation is 25.4%. The results show some size effect. As flexural depth increases, the ratio of test load to calculated load decreases.

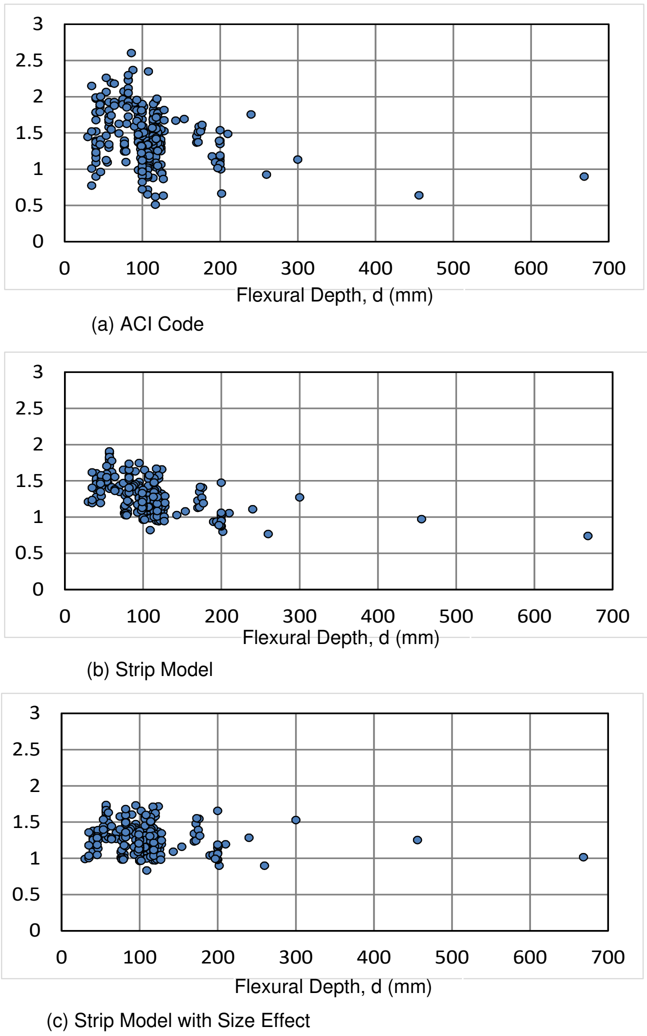

Figure 5: Ratio of test load to calculated load: concentric tests.

Figure 5(b) shows the same test results relative to calculated loads based on the Strip Model with no size effect considered. Here the average ratio of test load to calculated load is 1.24 with a coefficient of variation of 16.2%. While considerably less scattered than the results using the ACI code, there is still a noticeable trend to decreasing strength with increasing flexural depth.

To incorporate size effect with the Strip Model, one need only calculate the loading term, *w,* using an expression for one-way shear value that accounts for size. It is beyond the scope of this paper to present a detailed treatment of size effect. Instead, a simpler approach will be used. A size factor, $(a/d)^{\lambda}$, where a is a reference depth, d is the flexural depth of the slab, and λ is a fraction, will be incorporated in the loading term w.

The reference depth, a, is set to 100 mm (4 in). There are a couple of reasons for this choice. First, it is convenient. Second, it is approximately equal to the depth of the thinnest slabs that could still be considered full-scale.

Fujita et al. (2002) assess several methods that account for size effect in one-way shear and concluded that two separate populations were represented in their body of test results. For normal and medium strength concrete, they propose $\lambda = 1/4$. For high strength concrete specimens, they propose $\lambda = 1/2$. Since the expression for P_s places any size factor used in the expression for w under a second root sign, it follows that two-way shear is somewhat less sensitive to size than one-way shear. A compromise value of $\lambda = 1/3$ is used here. Revising the expression for w results in:

$$w = d \times 0.17\sqrt{f'_c} \times \sqrt[3]{\frac{100\,mm}{d}} \tag{8}$$

Figure 5(c) shows results ratios of test load to calculated load using the revised expression for w [Equation (8)] that accounts for size effect. The average ratio of test to calculated load for these 257 specimens is 1.24 and the coefficient of variation is 14.0%.

Some comments on the Strip Model:

- The Strip Model shows how a one-way shear limit combined with localized arching behavior is sufficient to explain two-way shear. A magnified "two-way" limiting shear stress is not necessary.
- With the loading term, w, held constant, the loaded length, l, increases with increasing flexural strength. In effect, the additional flexural capacity supports a larger "critical section."
- As presented above, the Strip Model has in no way been calibrated to the tests it is being used to analyze. The flexural strength of the radial strip is strictly that which can be attributed to a strip of slab with width defined by the supporting column. The loading term, w, is the one-way shear per unit width that one would use for a one-way slab. All the terms used in the Strip Model to calculate a two-way punching capacity are derived from one-way tests.
- Because the Strip Model makes use of only conventional flexural strengths and a one-way shear strength, it allows a unification of design treatment for one and two-way systems.
- The Strip Model does not describe a failure mechanism for a column-slab connection. It describes a load path that does not violate strength limits for flexure or one-way shear. With sufficient ductility in the system, the load predicted by the Strip Model is a lower bound of the capacity of the structure.

3 Connections transferring shear and moment

3.1 Proportional and non-proportional loading

To apply the Strip Model to the more general case of an interior connection under shear and moment requires a modified approach that does not rely on the level of symmetry usually found in concentric load tests. Most concentrically loaded test specimens reported in the literature have, more or less, four axes of symmetry in the distribution of slab curvature around the column. As is observed by Afhami et al. (1998), the loading is such that the nominal capacity of each radial strip is developed. This situation is called **proportional loading**. While most concentric load tests in the literature have this level of symmetry, most column-slab connections in practice do not.

Non-proportional, concentric loading occurs when the radial strips in one direction do not each their nominal capacity. The load is still concentric if there is no moment transferred to the column but the distribution of slab curvature around the column has only 2 axes of symmetry. The skew axes are no longer axes of symmetry. In this case enhanced radial strips will develop in one direction at the expense of strip development in the other. The limiting case, illustrated in Fig. 6, occurs when fully enhanced strips, each carrying a load P_{ss}, develop in one direction. The fully enhanced strip is called a super strip. Because radial strips do not develop in the direction perpendicular to the super strip, load transfer on the side face (c_1 face) of the column is limited to the one-way shear limit. The maximum total load transferred to the column with this load distribution is given by:

$$P_{col} = (\sum P_{ss}) + 2 \times w \times c_1 = 2 \times (P_{ss} + wc_1) \qquad (9)$$

This changed loading pattern requires some revision to the flexural capacity of the super strip. With non-proportional loading, the negative moment capacity of the strip need not be limited to the reinforcement within the strip. The radial super strip acts something like a T-beam in negative moment, with its "stem" defined column dimension perpendicular to the strip, c_2 and with a "top flange" wider than c_2.

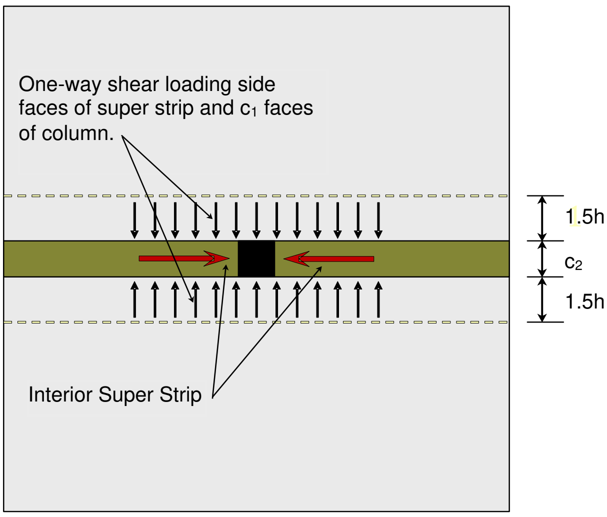

Figure 6: Non-proportional, concentric loading at interior connection.

Consistent with usual practice, it is assumed that top reinforcement within 1.5 times the slab thickness on either side of the column (i.e. within $c_2 + 3h$) is effective as top reinforcement for the radial super strip. Equation (6a) becomes:

$$M_{ss,neg} = \rho_{ss,neg} \times f_y \times j_{ss} \times c_2 \times d^2 \tag{10}$$

where $\rho_{ss,neg} = \rho_{neg} \times \frac{(c_2+3h)}{c_2}$

The factor j_{ss} is modified to account for flexural compression stresses framing into the side faces of the column joint. Alexander and Simmonds (2003) show that the effective width of the compression block associated with a wide band of flexural reinforcement is $c_1 + c_2$. For a super strip framing into a square or circular column, the gives:

$$j_{ss} = 1 - \frac{\rho \times f_y}{2 \times 1.7 \times f_c'} \tag{11}$$

The basic equations for loaded length and the total load carried are conceptually unchanged.

$$l_{ss} = \sqrt{\frac{M_{ss}}{w}} \tag{12}$$

$$P_{ss} = 2\sqrt{M_{ss}w} \tag{13}$$

Applying Equation (9) to the data set of 257 concentrically loaded test specimens results in an average test to calculated load of 1.24 with a coefficient of variation of 15.6%. In other words, the load path defined for non-proportional loading accounts for essentially the same load as proportional loading in the case of an interior column under concentric load. The virtue of considering this alternative load path is that it is more easily adapted to test specimen under eccentric loading.

3.2 Interior connections

The Strip Model allows the designer to assess independently the load coming into each face of a connection. Analogous to a shear failure in one of four beams framing into a column, punching occurs when one of these faces is overloaded. The net moment transferred to the connection is a consequence of the loading but not particularly relevant to the shear on any particular side of the connection. For example, in a continuous system with unequal spans, it is possible to design a connection that is not concentrically loaded yet transfers no moment to the column.

In contrast, for a test on an isolated column-slab connection, moment transfer is often the only measure of the degree to which one side of the connection is more heavily loaded. The following shows how the non-proportional load distribution developed above can be adapted to test specimens that meet at least one of two criteria: (1) the slab has the same reinforcing mats top and bottom and/or (2) the loading eccentricity is low enough to avoid load reversal.

Figure 7 shows a side view of an interior connection specimen under non-proportional, eccentric load. The load is treated as a combination of symmetric and anti-symmetric components. Punching occurs when one side of the connection reaches its limiting load.

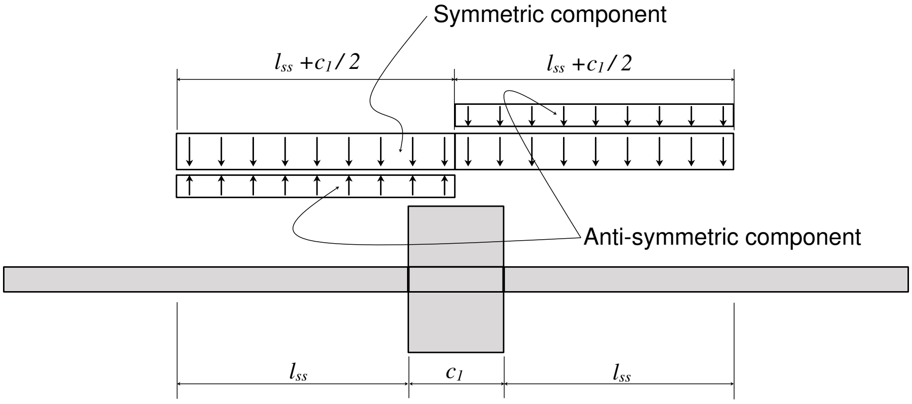

Figure 7: Simplified shear and moment transfer at interior connection.

The overall length of loading for the concentric component of load is $2l_{ss}+c_1$. The antisymmetric loading components are each distributed over half of this length, or $l_{ss}+c_1/2$. From equilibrium, the load distribution described in Fig. 7 results in:

$$\frac{P_{ult}}{2}+\frac{M_{ult}}{r}\leq P_{ss}+w\times c_1=2\times w\times r \tag{14}$$

where $r=l_{ss}+c_1/2$

The length r is analogous to a radius of gyration for the connection. The Strip Model makes this quantity dependent on the flexural reinforcement near the connection. The equivalent quantities in the ACI code are derived from geometric properties of a fixed critical section that is independent of reinforcement.

Tests by Hanson and Hanson (1968) and Hawkins et al. (1989) satisfy at least one of the two criteria listed earlier. Table 1 provides details for the 37 specimens considered here.

Hanson and Hanson (1968) tested 17 column-slab connections. Of these, seven specimens were of interior column-slab connections with solid slabs (no holes near the column) tested under combined shear and moment. All specimens had the same layout of reinforcement, top and bottom. Two loading methods are represented here. Type I loading involved the application of equal upward and downward line loads to the slab on either side of the column to produce high moment with little net vertical load transfer. Type III involved a single line load on one side of the column.

Hawkins et al. (1989) presents results from 30 tests of interior connections under eccentric loading. Point loads, controlled to produce a fixed eccentricity, were applied around the perimeter of the slab.

Table 2 provides test results as well as predicted failure loads using both the Strip Model [Equation (14)] and the ACI code. Both analyses give reasonable results although the limited size of the data set makes any statistical comparisons less compelling.